Combining EBV DNA dynamics with RECIST-based radiographic response to improve prognostic stratification of recurrent/metastatic nasopharyngeal carcinoma in the era of immunotherapy

Hao-Xang Long[1,#], Su-Chen Li[1,#], Cai-Rou Lai[2,#], Cheng-Long Huang[2,#], Xue-Song Sun[1], Bo-Wen Shen[1,3], Jia-Yi Shen[1,3], Hao-Jun Wang[1], Yi-Fu Li[1] Jie Chen[1], Hui Cheng[1], Li-Ting Liu[1], Qiu-Yan Chen[1,*], Hai-Qiang Mai[1,*], Lin-Quan Tang[1,2,*]

Rhinology 64: 4, 0 - 0, 2026
https://doi.org/10.4193/Rhin25.511

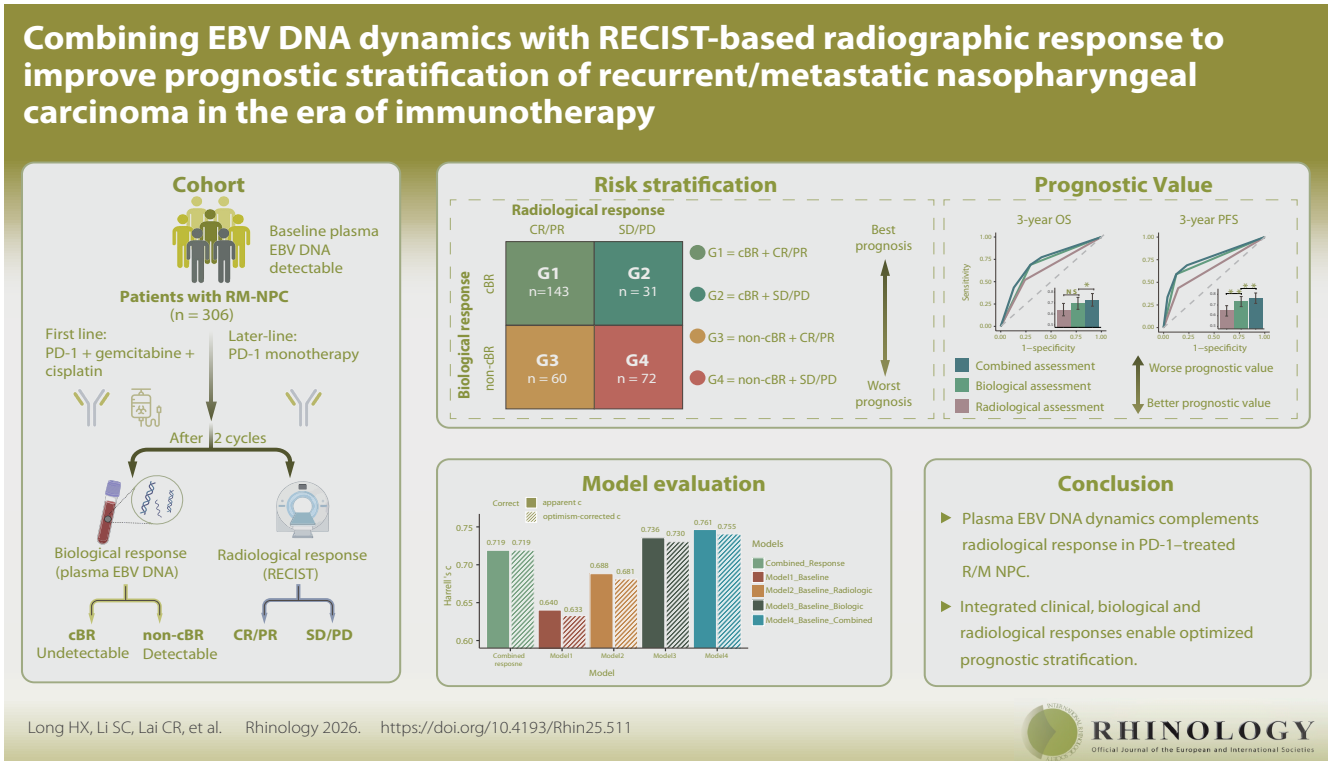

Abstract

Background: This study assessed the prognostic value of early Epstein–Barr virus (EBV) DNA dynamics combined with Response Evaluation Criteria in Solid Tumours (RECIST)-based radiographic response in patients with recurrent/metastatic nasopharyngeal carcinoma (R/M NPC) receiving immunotherapy, to refine risk stratification.

Methodology: A real-world cohort of 306 patients with R/M NPC and detectable EBV DNA at baseline received PD-1 monoclonal antibodies (PD-1 mAbs), alone or with chemotherapy. EBV DNA and radiological assessments were performed at baseline and after two therapy cycles. Biological responses based on EBV DNA were compared with RECIST evaluations. Survival outcomes were analysed using inverse probability treatment weighting, and a Cox regression model was developed incorporating baseline features and early responses.

Results: Among 306 patients, 174 achieved complete biological response (cBR), and 203 achieved complete or partial radiological response (CR/PR). Patients achieving both cBR and CR/PR had the most favourable progression-free survival. Early cBR was the dominant prognostic factor for overall survival, whereas radiological response did not affect overall survival within biological response strata. A prediction model integrating baseline features, radiological, and biological responses achieved an optimism-corrected C-index, surpassing models with baseline features alone, baseline plus radiological response, and baseline with biologi-

cal response.
Conclusions: Early biological response by EBV DNA was a stronger prognosticator than radiological response in PD-1 mAbs-treated R/M NPC. Combining baseline clinical features with biological and radiological responses improved survival prediction.

Key words: nasopharyngeal carcinoma, Epstein–Barr virus DNA, RECIST, immunotherapy, prognostic stratification

Introduction

Nasopharyngeal carcinoma (NPC) is endemic in southern China, southeast Asia, and north Africa, with a strong aetiological link to Epstein–Barr virus (EBV) infection [1-3]. Immunotherapy has transformed the management of recurrent or metastatic NPC (R/M NPC) [4-6]. Current National Comprehensive Cancer Network (NCCN) guidelines recommend anti-programmed cell death protein 1 monoclonal antibodies (PD-1 mAbs) combined with gemcitabine–cisplatin (GP) as first-line therapy or single agents in later treatment lines [7]. Nevertheless, a proportion of patients with R/M NPC derive little benefit from PD-1 mAbs. Identifying those at risk of resistance during treatment is therefore crucial for timely modification of therapeutic strategies.

Disease status is conventionally assessed using the Response Evaluation Criteria in Solid Tumours version 1.1 (RECIST v1.1) [4-6,8]. In the era of chemotherapy, early radiographic response was strongly correlated with survival in patients with metastatic NPC [9]. However, with immunotherapy, RECIST v1.1 may inadequately capture treatment response, particularly in the early phase [10]. Immune-related responses, including pseudoprogression and dissociated patterns, are linked to enhanced anti-tumour activity and may reflect inflammatory cell infiltration rather than true disease progression [11-14]. Indeed, patients categorised as progressing by RECIST but not by immune-adapted criteria (e.g., iRECIST) may achieve outcomes comparable with those who do not progress [11,12,15]. This underscores the need for complementary early-response modalities, such as liquid biopsy, which can dynamically reflect tumour burden and reveal treatment resistance at an early stage of PD-1 mAbs therapy for R/M NPC.

Plasma EBV DNA is a validated circulating biomarker for NPC [2]. Using ultrasensitive quantitative polymerase chain reaction (qPCR), cell-free EBV DNA fragments shed by tumour cells can be quantified in peripheral blood. Studies by Lv et al. demonstrated that dynamic EBV DNA changes during treatment provide valuable information for monitoring response and disease surveillance [16, 17]. Under chemotherapy, combining EBV DNA kinetics with radiographic assessments improved accuracy in evaluating tumour regression [18-20], highlighting the complementary value of biological response markers. Despite the limitations of RECIST during immunotherapy, early plasma EBV DNA declines remain predictive of long-term outcomes in patients with R/M NPC treated with PD-1 mAbs [21]. Thus, integrating EBV DNA kinetics with radiographic criteria may offer a reliable model for early response assessment.

Thus, this study aims to assess the prognostic and predictive significance of combining plasma EBV DNA kinetics with RECIST v1.1 during the early course of PD-1 mAbs treatment. Furthermore, we seek to establish a refined clinical prediction model incorporating EBV DNA decline, RECIST assessment, and baseline risk factors to optimise risk stratification and guide management of patients with R/M NPC receiving immunotherapy.

Materials and methods

Study population and data collection

Between January 2018 and February 2022, 306 patients with R/M NPC were identified at Sun Yat-sen University Cancer Centre. This study was approved by the Research Ethics Committee of Sun Yat-Sen University Cancer Centre (approval number: B2025-393).

Inclusion criteria were: 1) aged ≥18 and <75 years; 2) histologically confirmed WHO type II or III NPC; 3) stage IVb metastatic disease (eighth edition of the American Joint Committee on Cancer staging system for NPC) or local recurrence after curative locoregional radiotherapy (LRRT) not amenable to local treatment; 4) detectable plasma EBV DNA at baseline; 5) Eastern Cooperative Oncology Group performance status 0–1; 6) at least one measurable lesion by RECIST v1.1; and (7) receipt of ≥2 immunotherapy cycles.

Exclusion criteria were: 1) prior monoclonal antibody therapy against PD-1/PD-L1/CTLA4; 2) hepatic or renal insufficiency; 3) concurrent malignant disease, unless curatively treated >5 years earlier; 4) active or historical autoimmune disease; and 5) absence of plasma EBV DNA testing or radiological evaluation after two cycles.

Patients were retrospectively assigned to two cohorts based on treatment line. Patients that was treatment-naïve to R/M NPC formed the first-line cohort, while those with radiological progression after ≥1 platinum-based palliative chemotherapy regimen were assigned to the subsequent-line cohort.

Treatment protocol

Patients in the first-line cohort received GP combined with a PD-1 mAbs (tislelizumab, sintilimab, toripalimab, or camrelizumab) every 3 weeks (Q3W) for up to six cycles, followed by PD-1 mAbs monotherapy Q3W. In the chemotherapy phase, PD-1 mAbs was administered on day 1, gemcitabine (1,000 mg/m^2)

Table 1. Baseline characteristics.

Characteristic	n = 306
Age, years	
Median (IQR)	46 (38, 54)
Sex, n (%)	
Male	199 (65.0)
Female	107 (35.0)
ECOG score, n (%)	
0	188 (61.4)
1	118 (38.6)
Smoking history, n (%)	
No	194 (63.4)
Yes	112 (36.6)
Tumor stage, n (%)	
T0	107 (35.0)
T1	4 (1.3)
T2	14 (4.6)
T3	101 (33.0)
T4	80 (26.1)
Node stage, n (%)	
N0	126 (41.2)
N1	31 (10.1)
N2	46 (15.0)
N3	103 (33.7)
Metastasis stage, n (%)	
M0	32 (10.5)
M1	274 (89.5)
Bone metastasis, n (%)	
No	162 (52.9)
Yes	144 (47.1)
Liver metastasis, n (%)	
No	184 (60.1)
Yes	122 (39.9)
Lung metastasis, n (%)	
No	200 (65.4)
Yes	106 (34.6)
Distant LN metastasis, n (%)	
No	212 (69.3)
Yes	94 (30.7)
History of radiotherapy, n (%)	
No	168 (54.9)
Yes	138 (45.1)
Treatment line, n (%)	
1st line	239 (78.1)
subsequent line	67 (21.9)
Number of metastases, n (%)	
≤ 5	163 (53.3)
> 5	143 (46.7)
Baseline EBV DNA (copies/mL), n (%)	
≤ 7925	161 (52.6)
> 7925	145 (47.4)
PD-1 mAbs	
Camrelizumab	84 (27.5)
Tislelizumab	45 (14.7)
Toripalimab	158 (51.6)
Sintilimab	19 (6.2)

Abbreviations: ECOG, Eastern Cooperative Oncology Group performance status; LN, lymph node; EBV DNA, Epstein–Barr virus DNA.

on days 1 and 8, and cisplatin (80 mg/m^2) on day 1 of each cycle. Maintenance with PD-1 mAbs continued until disease progression, unacceptable toxicity, or a maximum of 2 years.

Patients in the subsequent-line cohort received PD-1 mAbs monotherapy on day 1 of each 3-week cycle, continued until radiographically confirmed progression, intolerable toxicity, or a maximum of 2 years.

Radiological assessment for tumour response

Radiographic imaging, including contrast-enhanced magnetic resonance imaging (MRI) of the nasopharynx and neck, and contrast-enhanced computed tomography (CT) scans of other body regions, was performed every two cycles to assess tumour response using RECIST v1 [8]. Complete response (CR) was defined as disappearance of all lesions; partial response (PR) as a ≥30% reduction in the sum of target lesion diameters; progressive disease (PD) as new lesions or a ≥20% increase; and stable disease (SD) as changes not meeting PR or PD criteria.

Biological assessment evaluated by plasma EBV DNA for tumour response

All patients underwent baseline plasma EBV DNA testing, followed by synchronous monitoring with radiological assessments during treatment. Quantification was conducted at Sun Yat-sen University Cancer Centre using the Sansure Biotech EBV DNA quantitative fluorescence diagnostic kit. The assay targeted the BamHI W fragment of the EBV genome, as described by Lo et al (22). Amplification was performed with the Applied Biosystems 7700 Sequence Detection System, and data were analysed using Sequence Detection Systems software (version 1.6.3). Each sample was tested in duplicate; if results differed by >10%, a third run was performed for validation.

Forward primer: 5'-CCCAACACTCCACCACACC-3';
Reverse primer: 5'-TCTTAGGAGCTGTCCGAGGG-3';
Probe sequence: 5'-(FAM)CACACACTACACACACCCACCCGTCTC(TAMRA)-3'.

Patients whose plasma EBV DNA levels fell below the assay's lower limit of detection (40 copies/mL) after two PD-1 mAbs treatment cycles were classified as having a complete biological response (cBR). Those with levels ≥40 copies/mL were classified as the non-cBR group.

Statistical analysis

The primary endpoint was progression-free survival (PFS), defined as the interval from treatment initiation to either radiographically confirmed PD or death. The secondary endpoint was overall survival (OS), measured from treatment initiation to death from any cause.

Continuous variables were expressed as medians with interquartile ranges, and categorical variables as frequencies and percentages. Between-group differences were evaluated using the chi-squared test. To address baseline imbalances, inverse probability of treatment weighting (IPTW) was applied before survival analyses [23,24]. The cut-off values for age and baseline EBV DNA copies was identified using maximally selected rank statistics, with PFS as the time-to-event outcome [25]. Survival distributions were estimated with the Kaplan–Meier method [26], and compared using log-rank tests. Hazard ratios (HRs) with 95% confidence intervals (CIs) were calculated using Cox proportional hazards regression [27]. Predictive accuracy of early-response assessment methods was evaluated by the area under the receiver operating characteristic curve (AUC), with CIs and statistical comparisons based on the DeLong method [28]. A clinical prediction model was built using Cox regression. Model discrimination was quantified by Harrell's C-index, corrected for optimism via 1000 bootstrap resamples [29]. Calibration was assessed using the Hosmer–Lemeshow goodness-of-fit test and calibration plots. Decision Curve Analysis (DCA) was conducted to evaluate the clinical net benefit of the prediction models across a range of threshold probabilities. Multiple comparisons were adjusted using the Benjamini–Hochberg (BH) method [30]. Statistical analyses were performed using R software (version 4.3.3). A two-tailed P value <0.05 was considered statistically significant.

Results

Baseline characteristics

A total of 306 patients with R/M NPC treated with PD-1 mAbs between January 2018 and February 2022 were included. Baseline characteristics are summarised in Table 1. The median age was 46 years (interquartile range [IQR] 38–54); 199 (65.0%) were male and 107 (35.0%) were female. Among them, 239 (78.1%) received GP+PD-1 mAbs as first-line therapy, while 67 (21.9%) received PD-1 mAbs monotherapy in subsequent lines. Radiological assessments were conducted after two treatment cycles, with EBV DNA surveillance performed at baseline and synchronously with imaging. By 25 May 2025, 218 progressions and 125 deaths had been recorded. Among the 125 deaths, 121 (96.8%) were due to tumour progression, 3 (2.4%) resulted from septic shock caused by neutropenic infection, and 1 (0.8%) was due to immune pneumonia. At a median follow-up of 33.5 months (IQR 22.4–48.0), the cohort had an mPFS of 16.3 months (95% CI 16.2–19.4) and an mOS of 56.3 months (95% CI 51.5–NR).

Early biological response and survival outcomes

All patients (n=306) presented with detectable baseline plasma EBV DNA (median 6,500 copies/mL; IQR 1,090–311,000 copies/mL). Patients with distant metastasis had higher EBV DNA levels than those with isolated locoregional relapse, and those with >5 metastatic lesions had higher levels than those with ≤5 (Figure S1). Maximally selected rank statistics identified 7,925 copies/mL as the prognostic cut-off. Patients with baseline EBV DNA >7,925 copies/mL had significantly poorer PFS than those with ≤7,925 copies/mL (HR=1.530, 95% CI 1.169–2.004, P=0.002; Figure S2). After two cycles, 174 of 306 patients (56.7%) achieved cBR, while 132 (43.1%) remained non-cBR. IPTW-adjusted analyses confirmed balance between groups (Table S1). Patients with cBR had significantly improved outcomes: mPFS was 33.5 months (95% CI 23.3–44.6) versus 9.6 months (95% CI 8.3–11.8) in non-cBR (HR=2.776, 95% CI 1.885–4.000, P<0.001; Figure 1A). The mOS for the cBR group was not reached, compared with 39.3 months (95% CI 30.2–NR) in non-cBR (HR=2.465, 95% CI 1.611–3.774, P<0.001; Figure 1B).

Radiological response and correlation with survival

After two immunotherapy cycles, RECIST evaluation classified 5 of 306 patients (1.6%) as CR, 198 (64.7%) as PR, 77 (25.2%) as SD, and 26 (8.5%) as PD. All patients with PD discontinued treatment at that time. For subsequent analyses, patients were grouped as CR/PR (objective response) or SD/PD (treatment resistance). Weighted survival analysis showed that the CR/PR group achieved a mPFS of 21.6 months (95% CI 17.0–32.7) compared with 10.2 months (95% CI 7.5–15.0) in the SD/PD group (HR=2.074, 95% CI 1.481–2.903, P<0.001; Figure 1C). Median OS was not reached in CR/PR, whereas the SD/PD group had a mOS of 38.7 months (95% CI 22.2–NR) (HR=1.675, 95% CI 1.038–2.700, P<0.001; Figure 1D).

Given potential heterogeneity between first-line and subsequent-line treatment cohorts, stratified analyses were performed. Consistent results were observed: cBR was associated with significantly longer mPFS and mOS compared with non-cBR, and CR/PR was superior to SD/PD in both treatment settings (Figure S3).

Coherence and differentiation between radiological and biological response

A significant correlation was found between radiological and biological responses (Chi-squared test, P<0.001). Of 306 patients, 143 (46.7%) achieved both CR/PR and cBR, while 72

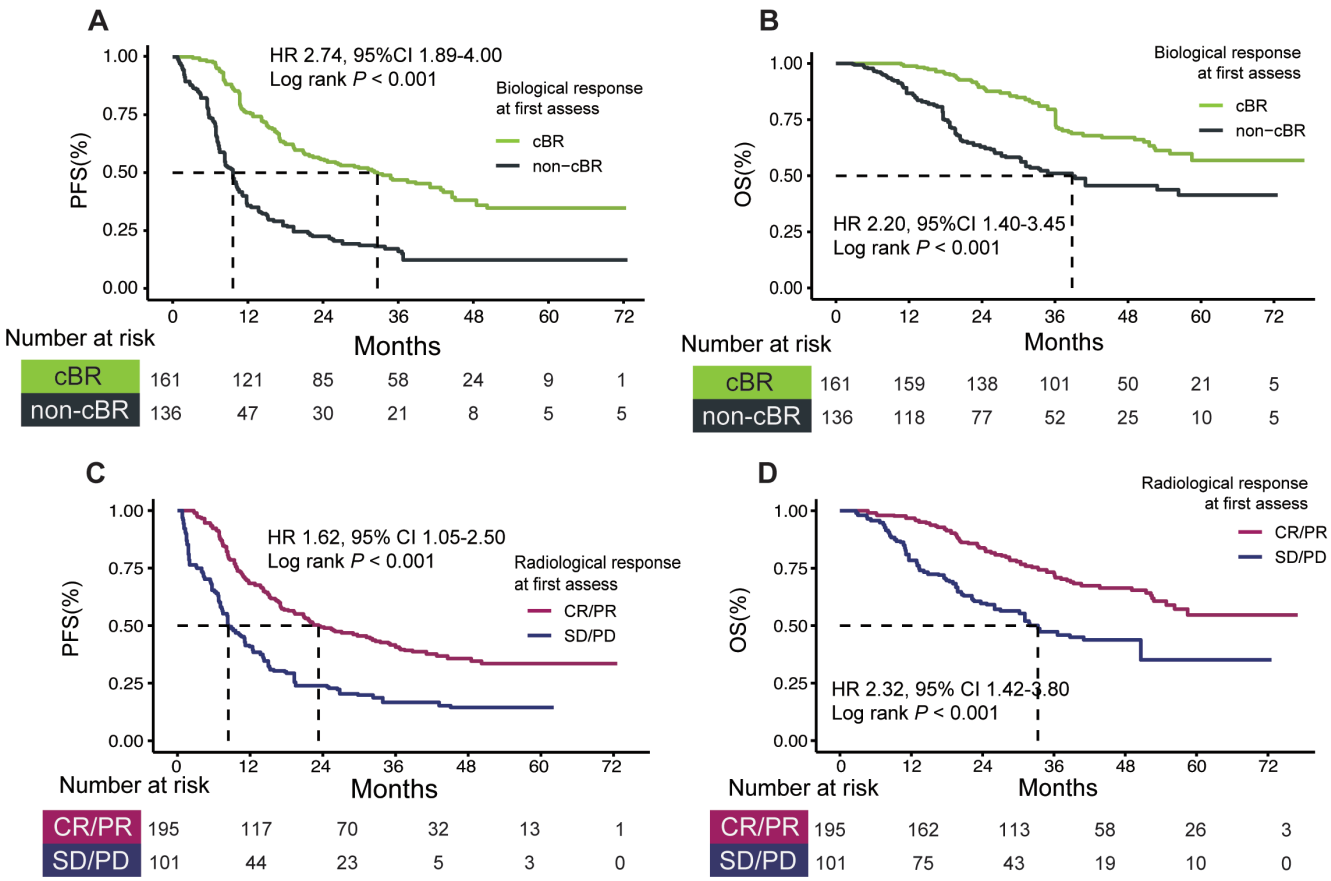

Figure 1. Relationship between first treatment response and prognosis. (A) PFS and (B) OS Kaplan–Meier curves for patients with cBR versus non-cBR after two treatment cycles. (C) PFS and (D) OS Kaplan–Meier curves for patients with CR/PR versus SD/PD after two cycles. Abbreviations: PFS, progression-free survival; OS, overall survival; cBR, complete biological response; HR, hazard ratio; 95% CI, 95% confidence interval; CR, complete response; PR, partial response; SD, stable disease; PD, progressive disease.

(23.5%) had both SD/PD and non-cBR. In line with a previous study [19], discrepancies were also noted: 31 patients (10.1%) achieved cBR despite radiological SD/PD, whereas 60 (19.6%) exhibited CR/PR but non-cBR. These findings suggest that EBV DNA kinetics may reflect biological changes that are not always in concordance with early imaging responses. Combining EBV DNA surveillance with RECIST therefore has potential to enhance early survival prediction. Accordingly, patients were classified into four response phenotypes based on radiological and biological assessments (Figure 2A): G1, cBR + CR/PR (n=143, 46.7%); G2, cBR + SD/PD (n=31, 10.1%); G3, non-cBR + CR/PR (n=60, 19.6%); and G4, non-cBR + SD/PD (n=72, 23.5%). Baseline clinical characteristics across phenotypes are summarized in the Figure S4. Notably, compared with the non-cBR phenotypes (G3/G4), patients in the cBR phenotypes (G1/G2) exhibited a lower number of metastases lesions, had a milder extent of distant lymph-node metastasis, and showed lower baseline EBV-DNA levels, whereas other metastatic patterns were largely comparable between the cBR and non-cBR phenotypes.

Combination of radiological and biological response better predict clinical outcome.

To evaluate the prognostic value of integrating radiological and biological responses, IPTW-corrected survival curves and hazard ratios were generated for the four phenotypes (Figures 2B–C). mPFS for G1, G2, G3, and G4 was 35.1 months (95% CI 23.6–51.5), 12.4 months (95% CI 8.3–24.7), 8.3 months (95% CI 6.9–15.2), and 7.5 months (95% CI 5.7–19.3), respectively. Median OS was not reached in G1 or G2, whereas it was 38.8 months (95% CI 26.1–NR) for G3 and 41.0 months (95% CI 17.5–NR) for G4. Among patients with favourable radiological response (G1 and G3), early biological response clearly differentiated outcomes: G3 had significantly worse survival than G1 (HRPFS=3.21, 95% CI 2.03–5.09, P<0.001; HROS=2.56, 95% CI 1.39–4.73, P<0.001). By contrast, among patients with unfavourable radiological response (G4 and G2), biological response did not significantly impact PFS (G4 vs. G2, HRPFS=1.60, 95% CI 0.86–2.90, P=0.058), though OS was markedly worse in G4 than G2 (HROS=3.15, 95% CI 1.27–7.80, P=0.002). When examining the role of radiological assessment within biological subgroups, differences were less

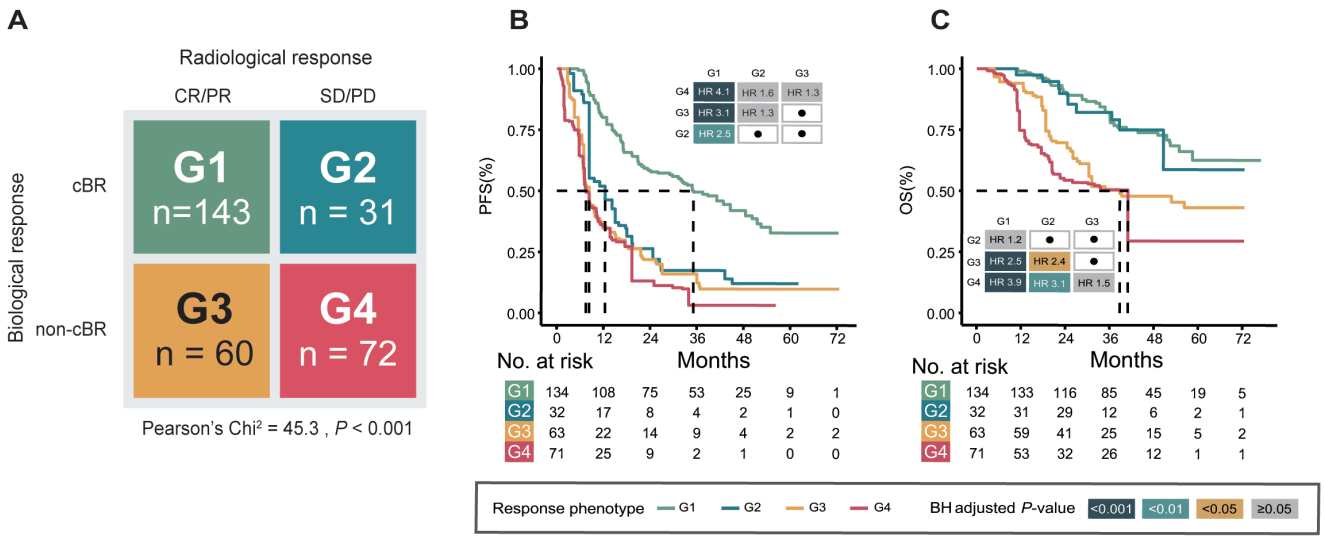

Figure 2. Combined survival analysis of imaging and biological assessment. (A) Cross-distribution of RECIST response (columns) and EBV DNA clearance (rows) at first efficacy evaluation in 306 patients. (B–C) IPTW-weighted Kaplan–Meier curves and pairwise hazard ratios for (B) PFS and (C) OS according to combined EBV DNA and RECIST response phenotypes: G1: Complete Biological Response (cBR) + CR/PR; G2, cBR + SD/PD; G3, non-cBR + CR/PR; G4, non-cBR + SD/PD. Abbreviations: EBV, Epstein–Barr virus; PFS, progression-free survival; OS, overall survival; BH, Benjamini–Hochberg method; CR, complete response; PR, partial response; SD, stable disease; PD, progressive disease; IPTW, inverse probability of treatment weighting.

consistent. Among patients achieving cBR, G2 had significantly shorter PFS than G1 (HRPFS=2.59, 95% CI 1.44–4.63, P<0.001), but OS did not differ (HROS=1.18, 95% CI 0.50–2.79, P=0.681). Among patients without cBR, no significant differences in PFS or OS were observed between G4 and G3 (HRPFS=1.25, 95% CI 0.76–2.07, P=0.260; HROS=1.47, 95% CI 0.78–2.77, P=0.118). Collectively, these results suggest that radiological assessments may be confounded by immune-related response patterns. Incorporating plasma EBV DNA dynamics provides complementary prognostic information, improving the accuracy of early response evaluation.

To validate our findings, we calculated 1-, 2-, and 3-year time-dependent AUCs for PFS and OS (Figure 3A–B). Across all time points, biological response demonstrated greater predictive accuracy than radiological response alone. For PFS, the combination of radiological and biological responses consistently outperformed either alone. At 1 year, the combination yielded an AUC of 0.779 (95% CI 0.727–0.830), superior to radiological response (0.647, 95% CI 0.584–0.700; P<0.001) and biological response (0.754, 95% CI 0.704–0.803; P=0.029). At 2 years, the combined AUC was 0.753 (95% CI 0.703–0.803), again exceeding radiological (0.638, 95% CI 0.588–0.687; P<0.001) and biological (0.725, 95% CI 0.677–0.773; P=0.016). At 3 years, the combined AUC remained highest at 0.763 (95% CI 0.715–0.812) versus radiological (0.646, 95% CI 0.597–0.694; P<0.001) and biological (0.732, 95% CI 0.685–0.779; P=0.008) (Figure 3A). Similar patterns were observed for the 1-, 2- and 3- year OS (Figure 3B). Collectively, these results confirm that integrating plasma EBV DNA dynamics with radiological assessment provides superior early prognostic accuracy compared with either method alone.

Establishment of clinical prediction models

Collectively, our findings demonstrate that combining biological and radiological responses during early treatment provides superior predictive value compared with either alone. A Cox model incorporating both responses achieved an apparent, optimism-corrected C-index of 0.719 for PFS prediction (Figure 4A), indicating robust prognostic utility. To approximate real-world clinical practice, we further developed four prognostic models integrating pretreatment and treatment-response features. Backward elimination identified ECOG performance status, baseline EBV DNA load, and number of metastatic lesions as independent prognostic factors for PFS (Table S2, Figure S5). These variables formed the basis of Model 1_Baseline. We then sequentially incorporated treatment response features to create three additional models: Model 2_Baseline_Radiologic (baseline + radiological response), Model 3_Baseline_Biological (baseline + biological response), and Model 4_Baseline_Combined (baseline + both radiological and biological responses). Corrected C-indices for these models are shown in Figure 4A. Model 1 achieved the lowest performance (0.633). Model 2 improved discrimination (0.681), while Model 3 further increased accuracy (0.730). Model 4 provided the highest predictive accuracy (0.755), significantly outperforming Model 1 (P<0.001) and Model 2 (P=0.042). Although Model 4 was not statistically superior to post-treatment response alone (0.755 vs. 0.719, P=0.170), its integration of readily available baseline features offers practical

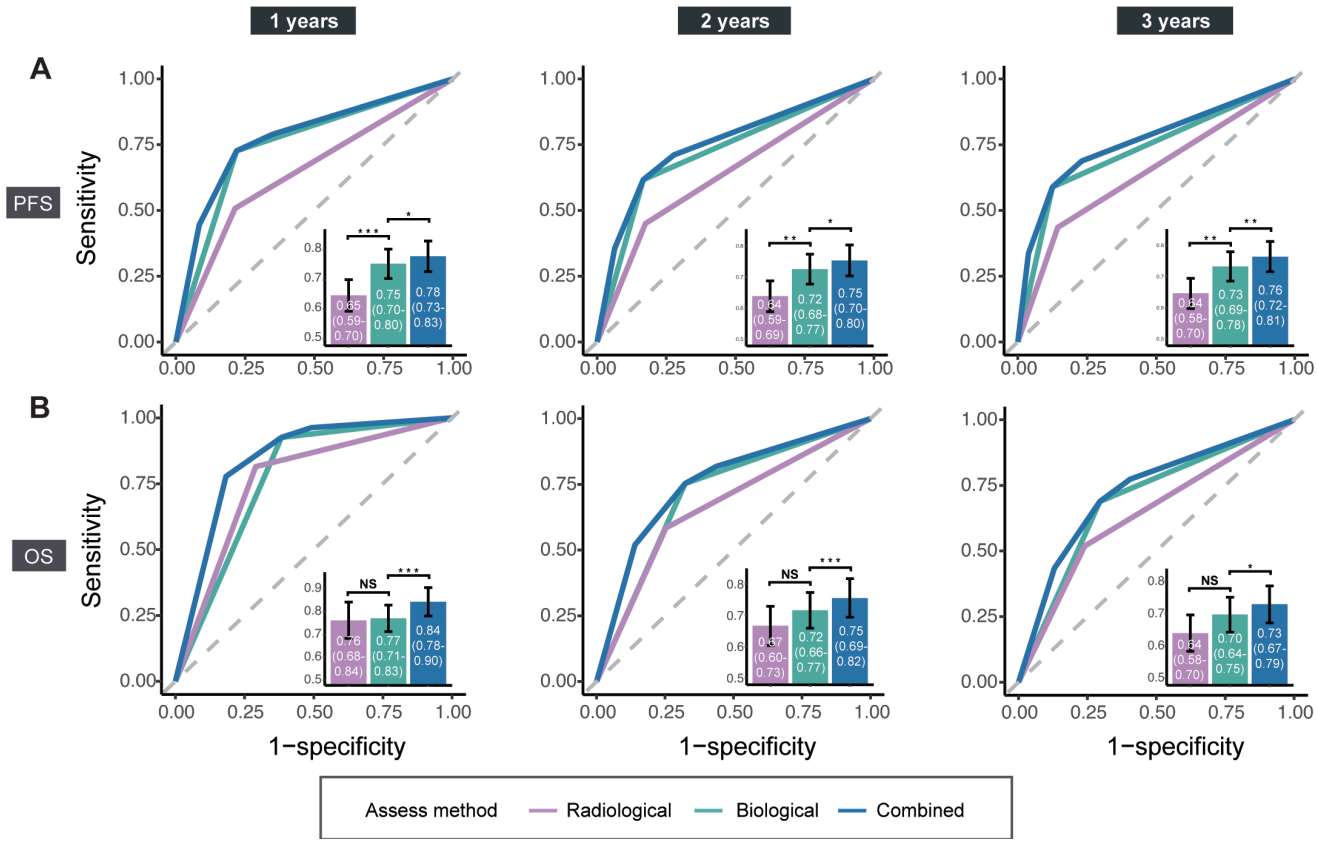

Figure 3. Time-dependent ROC curves for RECIST and EBV DNA in early treatment efficacy assessment. Assessment predicting 1-, 2- and 3-year (A) PFS and (B) OS. Abbreviations: PFS, progression-free survival; OS, overall survival; AUC, area under the curve; NS, not significant; ROC, receiver operating characteristic curve.

clinical value. Finally, a nomogram derived from Model 4 was constructed to estimate 1-, 2-, and 3-year PFS in patients with R/M NPC (Figure 4B). Calibration plots demonstrated excellent agreement between predicted and observed survival probabilities (Figure 4C). DCA at 1-, 2-, and 3-year timepoints showed that the Model 4 yielded the greatest net benefit across most threshold probabilities (Figure 4D; Figure S6). These findings suggest that incorporating both biological and radiographic responses offers improved clinical decision-making value.

Discussion

To our knowledge, this is the first study to systematically evaluate the combined prognostic value of radiological response, assessed by RECIST criteria, and biological response, assessed by EBV DNA kinetics, in patients with R/M NPC during early immunotherapy. Our findings demonstrate that biological response provides a robust complement to radiological evaluation, and that their integration yields superior predictive performance compared with either alone or with models based solely on baseline characteristics. Importantly, incorporating both radiological and biological responses with baseline clinical features produced the most accurate prediction model, supporting the use of combined response monitoring in future risk-adapted clinical trial designs and in guiding personalised therapeutic strategies for R/M NPC.

Pseudoprogression remains a critical challenge in the immunotherapy era. Although modified criteria such as iRECIST were developed to address this limitation, their dependence on serial imaging may delay clinical decisions and increase patient anxiety. The reproducibility of radiological measurements also poses difficulties [31], particularly in NPC, where tumour morphology is highly variable and complicates RECIST-based evaluation [19,32]. In this context, liquid biopsy provides a valuable adjunct, enabling earlier and potentially more accurate assessment of treatment response and prognosis [33]. There is growing interest in combining liquid biopsy with radiological response for refined risk stratification. In non-small cell lung cancer, melanoma, and urothelial carcinoma, ctDNA dynamics have shown strong concordance with best radiological response following immunotherapy [34-36]. In NPC, EBV DNA is released into the bloodstream through tumour cell death and reflects tumour burden, tumour biology, and potential occult metastasis [37-39]. The EP-SEASON study demonstrated that EBV DNA dynamics are closely associated with treatment response [17]. Furthermore, early declines in plasma EBV DNA titres predict long-term outcomes in patients with R/M NPC receiving immunotherapy [21]. Taken together,

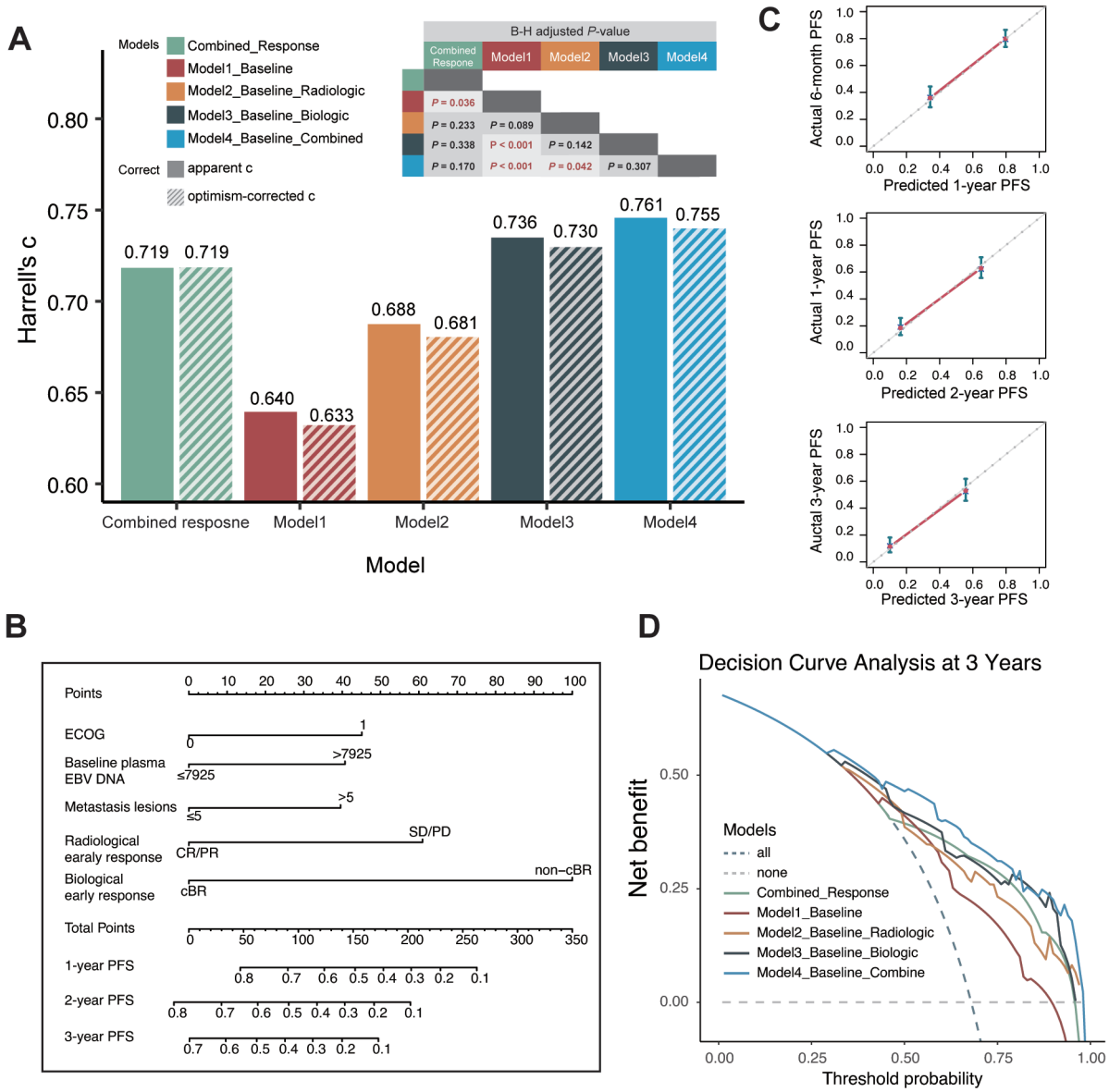

Figure 4. Development of models integrating baseline features. (A) Bar plot of apparent and optimism-corrected C-indices with pairwise comparisons of models incorporating baseline features, biological response, and/or radiological response using Cox proportional hazards models. (B) Nomogram estimating 1-, 2-, and 3-year PFS by integrating baseline features with radiological and biological response; overall points were matched to survival probabilities. (C) Calibration plots showing the actual risk probability by decile (y-axis) over the nomogram-predicted risk probability (x-axis). (D) Decision curve analysis (DCA) curves at 3 years. Abbreviations: PFS, progression-free survival; EBV, Epstein–Barr virus; ECOG, Eastern Cooperative Oncology Group performance status.

these findings highlight the clinical value of integrating EBV DNA kinetics with RECIST-based assessment to optimise patient management.

As our study demonstrated, stratification by biological response reveals an important nuance. Although patients with a radiological CR/PR generally showed superior OS compared with those with SD/PD, individuals achieving cBR had comparable long-term OS irrespective of radiological response category. Notably, their survival was significantly better than that of patients with radiological CR/PR who failed to achieve cBR. This divergence likely reflects the confounding effect of pseudoprogression on radiographic evaluation during immunotherapy. Accordingly, for patients achieving cBR despite radiological evidence of progression, caution is warranted against prematurely discontinuing treatment, as survival benefit may emerge over time. Conversely, failure to achieve cBR was associated with prognosis as poor as that of patients with SD/PD, even when radiological CR/PR was observed. This finding underscores the superior prognostic va-

lue of biological response compared with radiological response. EBV DNA assessment appears feasible as an early response indicator, particularly for patients without measurable disease under RECIST. However, radiological evaluation remains necessary. For patients with undetectable baseline EBV DNA, imaging provides the only means of treatment assessment. Moreover, EBV DNA testing lacks a standardised threshold for defining cBR, and a small proportion of patients may progress despite sustained EBV DNA clearance [40]. Sequential radiological monitoring, guided by iRECIST or similar criteria, therefore remains essential. Given the importance of tumour response rates as clinical endpoints, regular imaging retains considerable clinical value.

Despite the strong performance of dynamic indicators, baseline features such as ECOG, baseline EBV DNA load, number of metastatic lesions also carry important prognostic value [41-43]. Because these data are routinely available and incur no additional costs, we incorporated them with dynamic response information to construct our final model (Model4_Baseline_Combined). This integrative model provided superior predictive accuracy by synergistically combining static pre-treatment characteristics with post-treatment dynamics.

This study has several limitations. First, all patients in our cohort had detectable baseline EBV DNA. Although most patients with R/M NPC exhibit this feature due to greater tumour burden, strategies for evaluating biological response in those with undetectable EBV DNA require further exploration. Second, the lack of assay standardisation across platforms introduces variability in positivity thresholds, highlighting the need for validation with harmonised methodologies. Third, as a single-centre study, external validation in other institutions and non-endemic populations is warranted. Fourthly, heterogeneity in immunotherapy regimens may have introduced variability in treatment response. Meanwhile, differences in primary treatment approaches may also contribute to survival variability across patients. Finally, longer follow-up remains necessary to confirm OS outcomes and strengthen conclusions regarding the long-term prognostic value of our combined assessment strategy.

Conclusion

In summary, we demonstrated that early biological response assessed by plasma EBV DNA dynamics complements radiological response in patients with R/M NPC receiving PD-1 blockade. The integration of baseline clinical features with early biological and radiological responses yielded the strongest predictive performance for long-term survival, providing a practical framework for personalised treatment guidance.

Acknowledgements

ELSEVIER provided editing service to help with manuscript editing during drafting. The authors thank all participants who participated in this study and their families.

Author contributions

HXL, SCL, CRL and CLH contributed equally to this article. Concept and design: LQT, HQM and QYC. Acquisition, analysis, or interpretation of data: HXL, SCL, JYS and YFL. Drafting of the manuscript: HXL. Critical revision of the manuscript for important intellectual content: SCL, LTL and XSS. Statistical analysis: HXL, CLH, CRL, HC, JC and HJW. Administrative, technical, or material support: XSS, LTL. Supervision: LQT, HQM and QYC. All authors read and approved the final manuscript.

Conflict of interest

We declare no competing interests.

Funding

This study was funded by grants from the National Key Research and Development Program of China (2022YFC2505800, 2022YFC2705005), Noncommunicable Chronic Diseases-National Science and Technology Major Project (2024ZD0520706), National Natural Science Foundation of China (No. 82173287, 82372980, 82222050, 82303873, 32200651, 82203776, 82203125, 82272739, 82272882, 82373258, 82361168664, 82473396, 82473038), Guangdong Basic and Applied Basic Research Foundation (2023B1515120092), Science and Technology Program of Guangzhou (2023A04J1956, 2024B03J1248), Sun Yat-sen University Clinical Research 5010 Program (No. 2015021, 2017010), and China Postdoctoral Science Foundation (2024M763792).

Availability of data and materials

Data supporting the study findings are available on reasonable request to the corresponding author. The de-identified participant data will be securely deposited on the Research Data Deposit public platform (www.researchdata.org.cn). Researchers interested in using the data for scientific research purposes may request access through our corresponding author and database administrator.

References

1. Bray F, Laversanne M, Sung H, Ferlay J, Siegel RL, Soerjomataram I, et al. Global cancer statistics 2022: GLOBOCAN estimates of incidence and mortality worldwide for 36 cancers in 185 countries. CA Cancer J Clin. 2024;74(3):229–63.
2. Chen Y-P, Chan ATC, Le Q-T, Blanchard P, Sun Y, Ma J. Nasopharyngeal carcinoma. Lancet. 2019;394(10192):64–80.
3. Sun X-S, Liu S-L, Luo M-J, et al. The association between the development of radiation therapy, image technology, and chemotherapy, and the survival of patients with nasopharyngeal carcinoma: a cohort study from 1990 to 2012. Int J Radiat Oncol Biol Phys. 2019;105(3):581–90.
4. Yang Y, Qu S, Li J, et al. Camrelizumab ver-

sus placebo in combination with gemcitabine and cisplatin as first-line treatment for recurrent or metastatic nasopharyngeal carcinoma (CAPTAIN-1st): a multicentre, randomised, double-blind, phase 3 trial. Lancet Oncol. 2021;22(8):1162–74.
5. Mai H-Q, Chen Q-Y, Chen D, et al. Toripalimab or placebo plus chemotherapy as first-line treatment in advanced nasopharyngeal carcinoma: a multicenter randomized phase 3 trial. Nat Med. 2021;27(9):1536–43.
6. Yang Y, Pan J, Wang H, et al. Tislelizumab plus chemotherapy as first-line treatment for recurrent or metastatic nasopharyngeal cancer: a multicenter phase 3 trial (RATIONALE-309). Cancer Cell. 2023;41(6).
7. National Comprehensive Cancer Network. Head and Neck Cancers (Version 5.2025). Available from: http://www.nccn.org/professionals/physician_gls/pdf/head-and-neck.pdf [Accessed 12 August 2025].
8. Eisenhauer EA, Therasse P, Bogaerts J, et al. New response evaluation criteria in solid tumours: revised RECIST guideline (version 1.1). Eur J Cancer. 2009;45(2):228–47.
9. Liu G-Y, Li W-Z, Peng K-Q, et al. Prognostic value of early radiological response to first-line platinum-containing chemotherapy in patients with metastatic nasopharyngeal carcinoma. Cancer Med. 2020;9(3):920–30.
10. Cullen Q, Keshari KR. Imaging early response to checkpoint inhibition. Cancer Res. 2021;81(13):3444–5.
11. Wolchok JD, Hoos A, O'Day S, et al. Guidelines for the evaluation of immune therapy activity in solid tumors: immune-related response criteria. Clin Cancer Res. 2009;15(23):7412–20.
12. Seymour L, Bogaerts J, Perrone A, Ford R, Schwartz LH, Mandrekar S, et al. iRECIST: guidelines for response criteria for use in trials testing immunotherapeutics. Lancet Oncol. 2017;18(3):e143–e52.
13. Long GV, Weber JS, Larkin J, Atkinson V, Grob J-J, Schadendorf D, et al. Nivolumab for patients with advanced melanoma treated beyond progression: analysis of 2 phase 3 clinical trials. JAMA Oncol. 2017;3(11):1511–9.
14. Chiou VL, Burotto M. Pseudoprogression and immune-related response in solid tumors. J Clin Oncol. 2015;33(31):3541–3.
15. George S, Motzer RJ, Hammers HJ, et al. Safety and efficacy of nivolumab in patients with metastatic renal cell carcinoma treated beyond progression: a subgroup analysis of a randomized clinical trial. JAMA Oncol. 2016;2(9):1179–86.
16. Lv J, Chen Y, Zhou G, et al. Liquid biopsy tracking during sequential chemo-radiotherapy identifies distinct prognostic phenotypes in nasopharyngeal carcinoma. Nat Commun. 2019;10(1):3941.
17. Lv J, Xu L-X, Li Z-X, et al. Longitudinal on-treatment circulating tumor DNA as a biomarker for real-time dynamic risk monitoring in cancer patients: the EP-SEASON study. Cancer Cell. 2024;42(8).
18. Ma B, Hui EP, King A, et al. Prospective evaluation of plasma Epstein-Barr virus DNA clearance and fluorodeoxyglucose positron emission scan in assessing early response to chemotherapy in patients with advanced or recurrent nasopharyngeal carcinoma. Br J Cancer. 2018;118(8):1051–5.
19. Lv J, Wu C, Li J, et al. Improving on-treatment risk stratification of cancer patients with refined response classification and integration of circulating tumor DNA kinetics. BMC Med. 2022;20(1):268.
20. Liu Y, Yan W, Qi X, et al. Significance of longitudinal Epstein-Barr virus DNA combined with multipoint tumor response for dynamic risk stratification and treatment adaptation in nasopharyngeal carcinoma. Cancer Lett. 2024;605:217276.
21. Xu J-Y, Wei X-L, Ren C, et al. Association of plasma Epstein-Barr Virus DNA with outcomes for patients with recurrent or metastatic nasopharyngeal carcinoma receiving anti-programmed cell death 1 immunotherapy. JAMA Netw Open. 2022;5(3):e220587.
22. Lo YM, Chan LY, Lo KW, et al. Quantitative analysis of cell-free Epstein-Barr virus DNA in plasma of patients with nasopharyngeal carcinoma. Cancer Res. 1999;59(6):1188–91.
23. Xie J, Liu C. Adjusted Kaplan-Meier estimator and log-rank test with inverse probability of treatment weighting for survival data. Stat Med. 2005;24(20):3089–110.
24. Halpern EF. Behind the numbers: inverse probability weighting. Radiology. 2014;271(3):625–8.
25. Hothorn T, Lausen B. On the exact distribution of maximally selected rank statistics. Comput. Stat. Data Anal. 2003;43(2):121–37.
26. Bland JM, Altman DG. Survival probabilities (the Kaplan-Meier method). BMJ. 1998;317(7172):1572.
27. Cortese G, Holmboe SA, Scheike TH. Regression models for the restricted residual mean life for right-censored and left-truncated data. Stat Med. 2017;36(11):1803–22.
28. DeLong ER, DeLong DM, Clarke-Pearson DL. Comparing the areas under two or more correlated receiver operating characteristic curves: a nonparametric approach. Biometrics. 1988;44(3):837–45.
29. Iba K, Shinozaki T, Maruo K, Noma H. Re-evaluation of the comparative effectiveness of bootstrap-based optimism correction methods in the development of multivariable clinical prediction models. BMC Med Res Methodol. 2021;21(1):9.
30. Chen S-Y, Feng Z, Yi X. A general introduction to adjustment for multiple comparisons. J Thorac Dis. 2017;9(6):1725–9.
31. Casares-Magaz O, Raidou RG, Rørvik J, Vilanova A, Muren LP. Uncertainty evaluation of image-based tumour control probability models in radiotherapy of prostate cancer using a visual analytic tool. Phys Imaging Radiat Oncol. 2018;5:5–8.
32. Nishino M. Tumor response assessment for precision cancer therapy: response evaluation criteria in solid tumors and beyond. Am Soc Clin Oncol Educ Book. 2018;38:1019–29.
33. Gouda MA, Janku F, Wahida A, et al. Liquid biopsy response evaluation criteria in solid tumors (LB-RECIST). Ann Oncol. 2024;35(3):267–75.
34. Carvajal RD, Butler MO, Shoushtari AN, et al. Clinical and molecular response to tebentafusp in previously treated patients with metastatic uveal melanoma: a phase 2 trial. Nat Med. 2022;28(11):2364–73.
35. Anagnostou V, Ho C, Nicholas G, et al. ctDNA response after pembrolizumab in non-small cell lung cancer: phase 2 adaptive trial results. Nat Med. 2023;29(10):2559–69.
36. Passarella G, Canova S, Abbate MI, et al. The hype around ctDNA guiding an informed perioperative therapeutic strategy in early-stage non-small cell lung cancer. Discov Oncol. 2025;16(1):100.
37. Chan KCA, Zhang J, Chan ATC, et al. Molecular characterization of circulating EBV DNA in the plasma of nasopharyngeal carcinoma and lymphoma patients. Cancer Res. 2003;63(9):2028–32.
38. Fan H, Nicholls J, Chua D, et al. Laboratory markers of tumor burden in nasopharyngeal carcinoma: a comparison of viral load and serologic tests for Epstein-Barr virus. Int J Cancer. 2004;112(6):1036–41.
39. Ma BBY, King A, Lo YMD, et al. Relationship between pretreatment level of plasma Epstein-Barr virus DNA, tumor burden, and metabolic activity in advanced nasopharyngeal carcinoma. Int J Radiat Oncol Biol Phys. 2006;66(3):714–20.
40. Liu G-Y, Li W-Z, Xie C-B, Liang H, Xia W-X, Xiang Y-Q. Trajectories of EBV DNA and identifying the potential long-term survivors in metastatic nasopharyngeal carcinoma. Am J Cancer Res. 2021;11(8):3946–55.
41. Guo R, Tang L-L, Mao Y-P, et al. Proposed modifications and incorporation of plasma Epstein-Barr virus DNA improve the TNM staging system for Epstein-Barr virus-related nasopharyngeal carcinoma. Cancer. 2019;125(1):79–89.
42. Tang L-Q, Li C-F, Li J, et al. Establishment and validation of prognostic nomograms for endemic nasopharyngeal carcinoma. J Natl Cancer Inst. 2016;108(1).
43. Li S-C, Deng S-W, Sun X-S, et al. A new prognostic model for predicting outcomes of patients with recurrent or metastatic nasopharyngeal carcinoma receiving subsequent line (≥2 lines) anti-programmed death-1 monotherapy. Oral Oncol. 2023;139:106336.

Prof Lin-Quan Tang
Department of Nasopharyngeal Carcinoma
Sun Yat-sen University Cancer Centre
651 Dongfeng East Road
Guangzhou
Guangdong 510060
P. R. China

Tel: +86-20-8734-3643
Fax: 86-20-8734-339
E-mail: tanglq@sysucc.org.cn

Hao-Xang Long[1,#], Su-Chen Li[1,#], Cai-Rou Lai[2,#], Cheng-Long Huang[2,#], Xue-Song Sun[1], Bo-Wen Shen[1,3], Jia-Yi Shen[1,3], Hao-Jun Wang[1], Yi-Fu Li[1] Jie Chen[1], Hui Cheng[1], Li-Ting Liu[1], Qiu-Yan Chen[1,*], Hai-Qiang Mai[1,*], Lin-Quan Tang[1,2,*]

[1] Department of Nasopharyngeal Carcinoma, Sun Yat-sen University Cancer Centre, State Key Laboratory of Oncology in South China, Collaborative Innovation Centre for Cancer Medicine, Guangdong Key Laboratory of Nasopharyngeal Carcinoma Diagnosis and Therapy, Guangzhou 510060, Guangdong, China

[2] School of Biomedical Engineering, Southern Medical University, Guangzhou 510515, China

[3] Department of Anaesthesiology, Sun Yat-sen University Cancer Centre, State Key Laboratory of Oncology in South China, Guangdong Provincial Clinical Research Centre for Cancer, Guangzhou, China

[#] Contributed equally as joint first authors

[*] Contributed equally as joint corresponding authors

Rhinology 64: 4, 0 - 0, 2026
https://doi.org/10.4193/Rhin25.511

Received for publication:
October 10, 2025
Accepted: April 18, 2026

Associate Editor:
Basile Landis

This manuscript contains online supplementary material

SUPPLEMENTARY MATERIAL

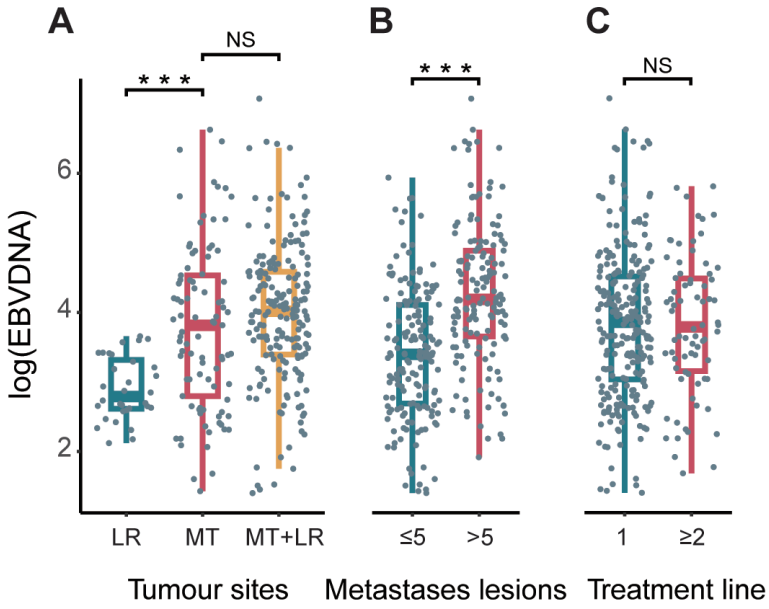

Figure S1. Characteristics of baseline EBV DNA(A) Box plot showing distributional differences in baseline EBV DNA across clinical parameters. (B) Kaplan–Meier survival plot of progression-free survival stratified by baseline EBV DNA load using the receiver operating characteristic-determined cut-off value. EBV DNA, cell-free Epstein–Barr virus DNA.

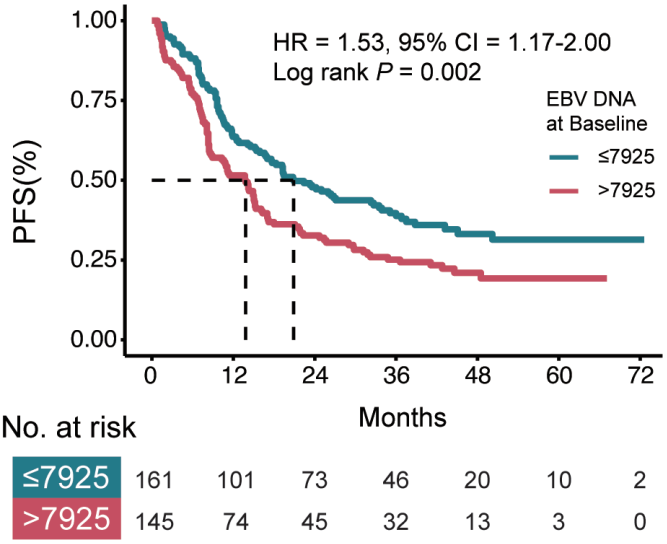

Figure S2. Kaplan–Meier survival curves for progression-free survival in high- versus low-burden baseline EBV DNA groups. EBV DNA, cell-free Epstein–Barr virus DNA.

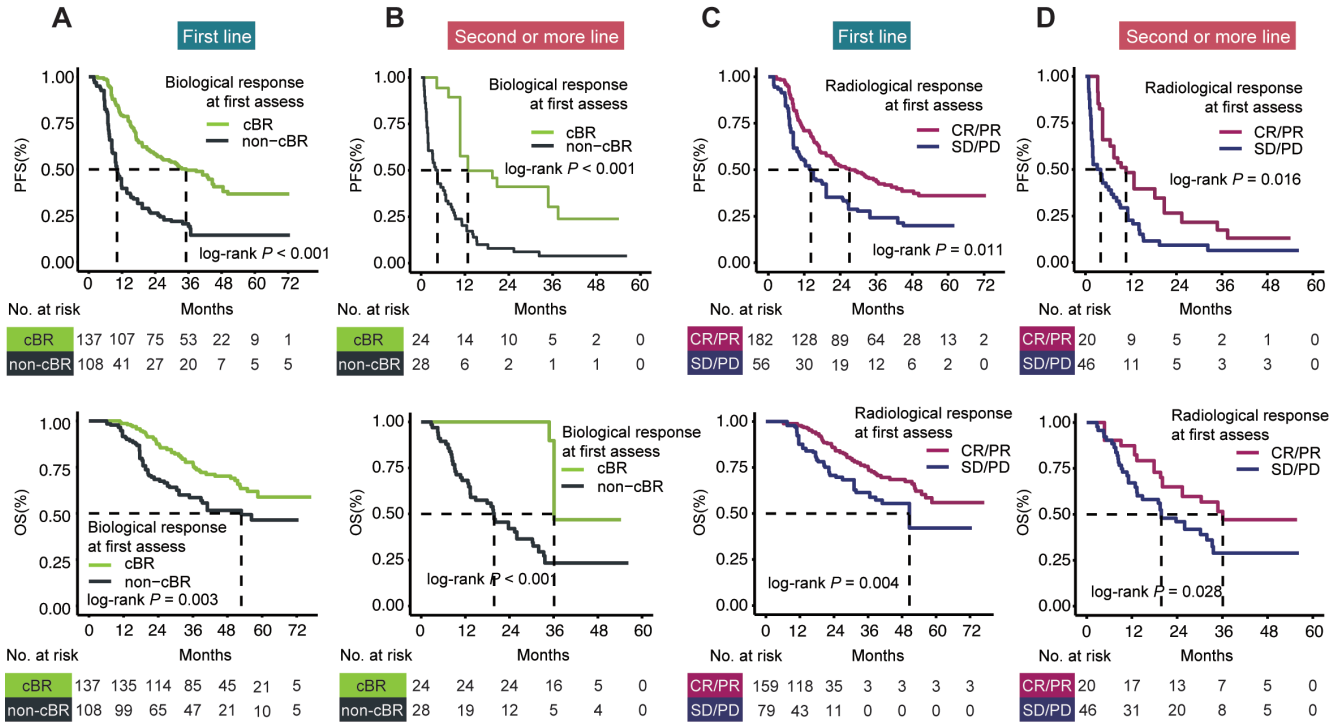

Figure S3. Relationship between Imaging Response and PFS and OS in Patients with different treatment lines. Kaplan–Meier survival curves: (A) first-line patients and (B) second-line or later patients achieving cBR/non-cBR at the first efficacy evaluation; Kaplan–Meier survival curves for (C) first-line patients and (D) second-line or later patients achieving SD/PD and CR/PR at the first efficacy evaluation. Abbreviations: PFS, progression-free survival; OS, overall survival; cBR, complete biological response; HR, hazard ratio; 95% CI, 95% confidence interval.

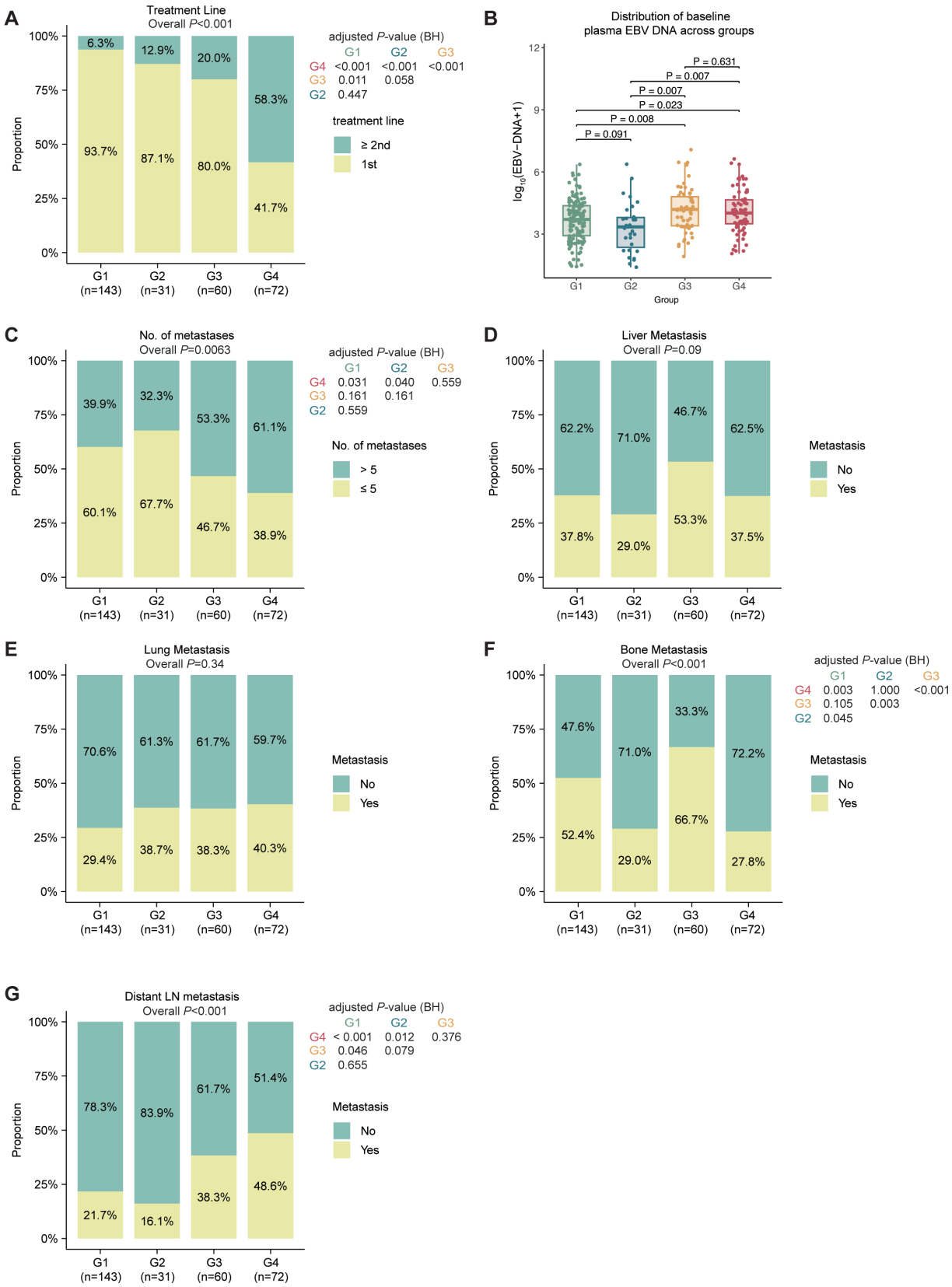

Figure S4. Baseline clinical characteristics across the G1, G2, G3, and G4 phenotypes. (A) Stacked bar chart of treatment line distribution. (B) Boxplot of baseline log-transformed plasma EBV-DNA levels. (C–G) Stacked bar charts showing metastatic patterns: (C) number of metastases, (D) liver metastasis, (E) lung metastasis, (F) bone metastasis, and (G) distant lymph-node metastasis. For stacked bar charts, an overall chi-square test was first performed. When the overall P value was <0.05, post-hoc chi-square tests were conducted between groups with BH correction for multiple comparisons.

Variable		N	Hazard ratio	p
Baseline plasma EBV DNA	≤ 7925	161	Reference	
	>7925	145	1.83 (1.38, 2.42)	<0.001
ECOG	0	188	Reference	
	1	118	1.74 (1.33, 2.29)	<0.001
Number of metastasis leasions	≤ 5	163	Reference	
	> 5	143	1.60 (1.21, 2.12)	0.001

Figure S5. Baseline independent predictors of risk factors for progression-free survival identified by backward elimination.

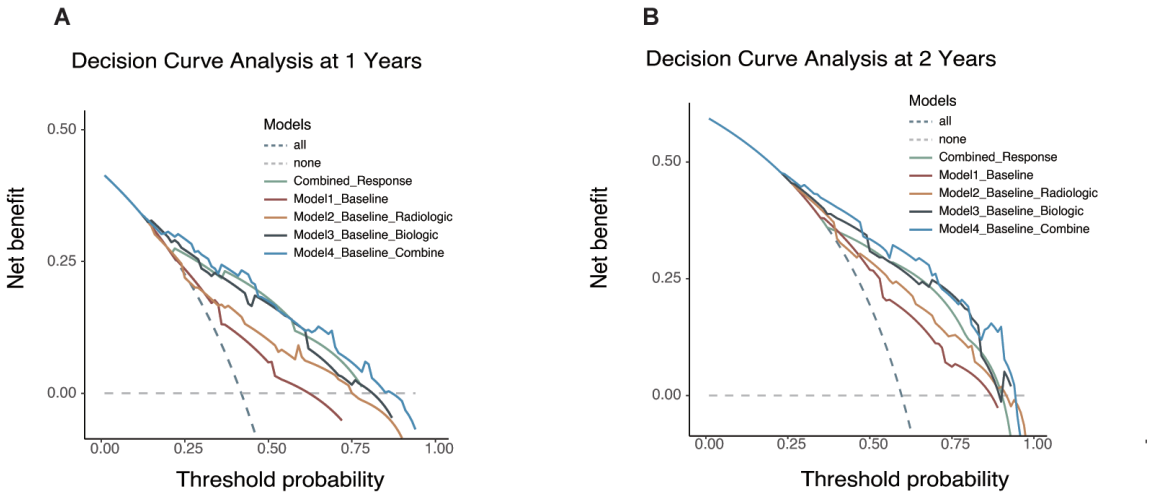

Figure S6. Decision curve analysis (DCA) curves at 1 year (A) and 2 years (B).

Table S1. P-values comparing baseline characteristics between subgroups in the unadjusted and inverse probability of treatment weighting (IPTW)-adjusted cohorts.

	Radiological response		Biological response		Response phenotypes	
	UN	IPTW [a]	UN	IPTW [b]	UN	IPTW [a]
Age	0.124	0.059	0.904	0.747	0.257	0.206
Sex	0.700	0.865	0.520	0.968	0.868	0.100
ECOG	<0.001	0.929	0.001	0.453	0.053	0.238
Smoking	0.192	0.797	0.964	0.402	0.429	0.176
T stage	0.081	0.815	0.306	0.369	0.512	0.377
N stage	<0.001	0.852	0.236	0.807	0.052	0.508
M stage	0.042	0.972	0.739	0.810	0.013	0.320
Bone metastases	<0.001	0.791	0.708	0.979	<0.001	0.493
Liver metastases	0.259	0.173	0.166	0.968	0.090	0.279
Lung metastasis	0.220	0.235	0.161	0.383	0.3401	0.104
Distant lymph metastases	0.039	0.702	<0.001	0.595	<0.001	0.327
History of radiotherapy	<0.001	0.946	0.166	0.989	0.001	0.414
Lines	<0.001	0.872	<0.001	0.353	<0.001	0.481
Number of metastases	0.193	0.075	0.001	0.906	0.006	0.259
Pre-treatment plasma EBV DNA	0.256	0.182	0.003	0.983	<0.001	0.386

Abbreviations: EBV DNA Cell-free Epstein-Barr virus DNA; ECOG Eastern Cooperative Oncology Group performance status; UN unadjusted, IPTW inverse probability treatment weighting. [a] Adjusted by the IPTW algorithm: ECOG (0 vs. 1), smoking (No vs. Yes), N stage (N0 vs. N1 vs. N2 vs. N3), M stage (M0 vs. M1), bone metastasis (No vs. Yes), distant lymph metastasis (No vs. Yes), history of radiotherapy (No vs. Yes), treatment lines (first line vs. subsequent line), metastatic lesion count (≤5 vs. >5). [b] Adjusted by the IPTW algorithm: ECOG (0 vs. 1), M stage (M0 vs. M1), distant lymph metastases (No vs. Yes), treatment lines (first line vs. subsequent line), Number of metastases (≤5 vs. >5), pre-treatment plasma EBV DNA (≤7925 copies/mL vs. >7925 copies/mL). [c] Adjusted by the IPTW algorithm: age (≤46 vs. >46), ECOG (0 vs. 1), T stage (T0 vs. T1 vs. T2 vs. T3 vs. T4), N stage (N0 vs. N1 vs. N2 vs. N3), M stage (M0 vs. M1), bone metastases (No vs. Yes), liver metastases (No vs. Yes), distant lymph metastases (No vs. Yes), history of radiotherapy (No vs. Yes), treatment lines (first line vs. subsequent line), Number of metastases (≤5 vs. >5), pre-treatment plasma EBV DNA (≤7925 copies/mL vs. >7925 copies/mL). Abbreviations: EBV DNA, cell-free Epstein–Barr virus DNA; ECOG, Eastern Cooperative Oncology Group performance status; UN, unadjusted; IPTW, inverse probability of treatment weighting.

Table S2 Univariate and multivariate analyses for the clinical nomogram.

Characteristic	Univariate		Multivariate [a]	
	HR(95% CI)	P-value [b]	HR (95% CI)	P-value [b]
Age				
≤ 46	Reference		Reference	
> 46	1.26(0.97-1.65)	0.085	1.15(0.87-1.54)	0.323
Sex				
Female	Reference			
Male	0.88 (0.66-1.17)	0.383		
Smoking				
No	Reference			
Yes	1.16 (0.89 - 1.53)	0.272		
ECOG				
0	Reference		Reference	
1	1.90(1.45 - 2.49)	<.001	1.73 (1.31 - 2.30)	<.001

Characteristic	Univariate		Multivariate [a]	
	HR(95% CI)	P-value [b]	HR (95% CI)	P-value [b]
T stage				
T0	Reference			
T1	0.51 (0.19 – 1.39)	0.187	0.60 (0.22 – 1.67)	0.327
T2	1.08 (0.59 – 1.99)	0.793	1.42 (0.77 - 2.64)	0.261
T3	0.76 (0.55 - 1.04)	0.090	0.81 (0.58 - 1.14)	0.228
T4	0.92 (0.65 - 1.30)	0.637	0.86 (0.60 - 1.24)	0.422
N stage				
N0	Reference			
N1	0.69 (0.41 - 1.14)	0.143		
N2	0.82 (0.55 - 1.22)	0.328		
N3	0.91 (0.67 - 1.23)	0.538		
M stage				
M0	Reference			
M1	1.15 (0.73 – 1.81)	0.532		
Bone metastasis				
No	Reference			
Yes	0.13 (0.863 - 1.47)	0.379		
Lung metastasis				
No	Reference		Reference	
Yes	1.53 (1.17 – 2.01)	0.002	1.18 (0.87 - 1.60)	0.278
Liver metastasis				
No	Reference		Reference	
Yes	1.92 (1.45 – 2.53)	<.001	1.23 (0.88 - 1.60)	0.278
Distant LN metastasis Lesions				
No	Reference		Reference	
Yes	1.27 (0.967 – 1.65)	0.086	0.92 (0.67 - 1.25)	0.578
Baseline EBV DNA				
≤ 7925 copies/mL	Reference		Reference	
> 7925 copies/mL	1.51 (1.16 - 1.96)	<.001	1.78 (1.34 – 2.37)	<.001
Number of metastases				
≤ 5	Reference		Reference	
> 5	1.74 (1.34 - 2.27)	<.001	1.50 (1.07 – 2.11)	0.020
History of LRRT				
No	Reference			
Yes	1.17 (0.90 – 1.53)	0.246		

[a] Only variables with P-values <0.1 in univariate analyses were included. [b] Tests performed using the Cox proportional hazards model. Abbreviations: CI, confidence interval; OS, overall survival; EBV DNA, cell-free Epstein–Barr virus DNA; ECOG, Eastern Cooperative Oncology Group performance status; UN, unadjusted; LRRT, locoregional radiotherapy.